Reactive Transport of CO_2 in a Brine Cavity

By Meredith Hill and Dirk Van Essendelft

ABSTRACT

Saline aquifers are viable geologic sinks for the sequestration of CO_2. The sequestration behavior was modeled within a two-dimensional square of 1 meter on a side in COMSOL 3.2. The advection-diffusion, Navier-Stokes, and advection-conduction equations were coupled to model the fluid behavior of the reaction, concentration body forces, and thermal body forces. Reasonable behavior was attained, however, time and computing resources did not allow for the use of the actual diffusion and thermal conductivity constants. These constants were too low for the mesh size, and the small mesh size needed created computational needs that exceeded what was available at this time. Nevertheless, there is reason to believe that given more resources, the real behavior could be measured.

INTRODUCTION

Mean annual concentrations of gaseous CO_2 have increased by 19.4% from 315.98 parts per million by volume (ppmv) of dry air in 1959 to 377.38 ppmv in 2004.[1] Sequestering CO_2 within saline aquifers is a viable method to store this gaseous CO_2 that would otherwise be released to the earth's atmosphere since they are geographically abundant and located in close proximity to industrial emission sources.[2-10] Saline aquifers are also rich in Ca^{2+}, Mg^{2+}, Fe^{2+}, and Sr^{2+}; all of which can be converted into stable carbonates through sequestration.[11, 12] Since saline aquifers naturally exist at environments other than standard conditions (i.e., increased temperatures, pressures, and salinities), it is necessary to consider and predict how this range of conditions contributes to the physico-chemical behavior of gaseous CO_2 after injection.[13-15] The geochemical processes occurring once CO_2 is injected into the reservoir's subsurface include solubility trapping (i.e., the dissolution of some of this injected CO_2 into $CO_{2(aq)}$), hydrodynamic trapping (i.e., the existence of CO_2 as an immiscible plume), and mineral trapping (i.e, converting or precipitating dissolved CO_2 into stable carbonate minerals).[16, 17] Saline aquifers are estimated to store 10s – 1000s Gigatons of Carbon.[18] Dissolved and immiscible CO_2 have residence times ranging from 1 million to millions of years, respectively. Solubility trapping will be modeled initially, and if time allows, modeling of mineral trapping will follow.

The intention is to model the saline aquifer as a container of simple geometry (i.e., a cube). The geometry of a real aquifer will affect the fluid behavior, however a simple case can illustrate a great deal about the basics of fluid behavior in a given system. Supercritical CO_2 is not completely miscible in aqueous solutions and is less dense than the saline solutions. Thus, the injection will be modeled by setting the top boundary of the system at a constant CO_2 concentration equal to that of the maximum solubility at appropriate reservoir pressures and temperatures. It is also known that the density of saline-CO_2 solutions vary according to temperature, pressure, and CO_2 concentration.[6, 11, 13-15, 17] The solutions become more dense with higher CO_2 content.[19] Finally, reactions can occur in the solution and, in doing so, release heat.[17] The goal of this project is to incorporate all of these effects into one model to gain

insight into the behavior of this system over time. The modeling will occur in a series of steps. First, the diffusion of CO_2 will be modeled using constant density and the diffusion equations.[19-21] Next, the effects of CO_2 concentration and pressure on fluid density will be modeled and applied to the fluid mechanics equations. This will add convection to diffusion. Finally, a sink term will be added to the mass balance equations, a heat generation term will be added to the energy equations proportional to the sink term, and the temperature effects on density will be added[22] – This should model reaction within the system. These outlined steps should yield a model that is relatively accurate and attainable within the bounds of this course.

GOVERNING EQUATIONS

The system can be modeled by coupling three differential equations: the advection-diffusion equations for each component (salt and CO_2), the Navier-Stokes equations, and the advection-conduction equation.

The first approximation will involve solving the diffusion equation for constant density and no reaction. The equations are as follows:

$$\frac{\partial c_i}{\partial t} = \nabla J_i \qquad (1)$$

The constitutive relationship for this approximation is Fick's first law: $J_i=D\nabla c_i$. c_i refers to the concentration of any species in solution and D is the diffusion coefficient. For our system, we will consider both carbon dioxide and a given salt, so there will be two simultaneous diffusion equations. ∇J_i is the flux of c_i into and out of a differential element by diffusion. The boundary conditions for this approximation are constant concentration along the top boundary equal to that of the maximum solubility. All other boundaries will be no flux boundaries. The initial condition will be that there is no CO_2 within the fluid volume.

The second approximation will be to make the bulk fluid density a function of concentration. This means that density differences will drive fluid motion, thus there is a need to add the motion equations and couple them to the diffusion equations as follows:

$$\frac{\partial(\rho v)}{\partial t} + \nabla \cdot \rho v v = -\nabla P + \nabla \tau \qquad (2)$$

$$\frac{\partial c_i}{\partial t} = \nabla J_i - v\nabla c_i \qquad (3)$$

where v is the velocity vector, ρ is the bulk density, P is the total pressure, τ is the stress tensor defined by Newton's law $\tau=\mu\nabla v$, μ is the dynamic viscosity and $v\nabla c_i$ is the flux into and out of a differential element by convection. Furthermore, the mass balance gives $\nabla v=0$. In addition to the boundary conditions for diffusion, all boundaries will have a no-slip condition imposed, and pressure will only be a function of gravity and the top boundary pressure. The initial conditions will be that $v=0$ within the volume.

The final approximation is to add reaction and energy balance to the system and make density a function of concentration, temperature, and pressure. This changes the diffusion equation to:

$$\frac{\partial c_i}{\partial t} = D\nabla^2 c - v \cdot \nabla c_i + R_i \qquad (4)$$

where R_i is the reaction rate expression for a given constituent. The energy balance becomes:

$$C_p\left(\frac{\partial(\rho T)}{\partial t}+\nabla\cdot\rho vT\right)=\nabla q-\left(\frac{\partial\ln(\rho)}{\partial\ln(T)}\right)_p\frac{DP}{Dt}-(\tau:\nabla v)+H_rR_i \qquad (5)$$

where C_p is the heat capacity and H_r is the molar heat of reaction. It can be assumed that the viscous dissipation heating effects are negligible, because the velocities are low, and that density is a weak function of temperature. The constitutive equation for the energy balance is Fourier's law: $q=\kappa\nabla T$. Combining the assumptions and the constitutive equation yields:

$$C_p\left(\frac{\partial(\rho T)}{\partial t}+\nabla\cdot\rho vT\right)=\kappa\nabla^2T+H_rR_i \qquad (6)$$

The boundary and initial conditions do not change for the diffusion and fluid motion equations. The thermal boundary conditions are constant temperature, and the initial conditions will be the temperature at the relevant aquifer depth.

SOLUTION

CO_2 sequestration within a saline aquifer was modeled using COMSOL 3.2. The geometry was represented by a 2-D square with dimensions of 1 meter on each side. Physical values for the system were obtained from the literature, or reasonably assumed, and applied to the system (Tables 1-4). The highlighted values (in bold-italics) in Table 3 were chosen to allow the system to converge to a stable solution within reasonable computational time. Given more computing resources, realistic values and a representative geometry could have been implemented within a reasonable timeframe. The mesh size would also have to be considerably reduced in size. The actual values for the diffusion coefficient and the thermal conductivity are on the order of $1x10^{-9}$ m^2/s[23] and 0.6062 W/(m*K)[24], respectively. In addition, the reaction was found to be a complicated surface governed reaction, which is not easily modeled[25]. Therefore, the reaction was modeled as an elementary first order reaction in both c and c2. The overall reaction can be expressed as $R=k[CO_2][brine]$. The reaction constant, k, was estimated from the literature and adjusted so that a reasonable solution could be obtained.

Table 1
Simulation Boundary Conditions

Boundary Conditions	**Value**
Insulation/No slip unless otherwise specified	--
Constant Temperature Boundary (K) – All Boundaries	358*
Concentration of CO_2 (mol/m^3) – Top Boundary	627.55 [26]
Point Pressure (Pa) – Top Boundary	7584233*

*Temperature and pressure boundary conditions are representative of an 800m deep reservoir

Table 2
Simulation Initial Conditions

Initial Conditions and units	**Value**	**Symbol**
Concentration of CO_2 (mol/m^3)	0	C
Concentration of brine (mol/m^3)	4000	c2
Velocity Field (m/s)	0	--
Initial Temperature (K)	358	To

Table 3
Data Input for the Simulation

Data Constants and units	Value	Symbol
Bulk Solution Density (kg/m^3)	1000	rho_s
Gravitational Constant (m/s^2)	9.81716	g
Diffusion Coefficient of CO2 (m^2/s)	***0.00005***	diff
Reaction Rate Constant (1/mol*s*m^3)	***1.00E-06***	k1
Thermal Conductivity (W/m*K)	***100000***	tc1
Heat of Reaction (J/mol)	1341120**	Hrxn
Thermal Expansion Coefficient (1/K)	0.000695 [27]	alpha
Time Scaling Coefficient	0.01667	dts
Heat Capacity (J/kg*K)	4186	Cpw

**Calculated for calcite

Table 4
Fundamental Equations for Simulation

Description	Expression	Symbol
Solution Density with CO_2	rho_s+c*17.75/1000 [28]	rho_c
Bouyant Force	-(rho_c-rho_s)*g+rho_c*g*(T-To)*alpha	Fb
Gravitational Force	-rho_c*g	Fg
Reaction Rate	-k1*c*c2	rate

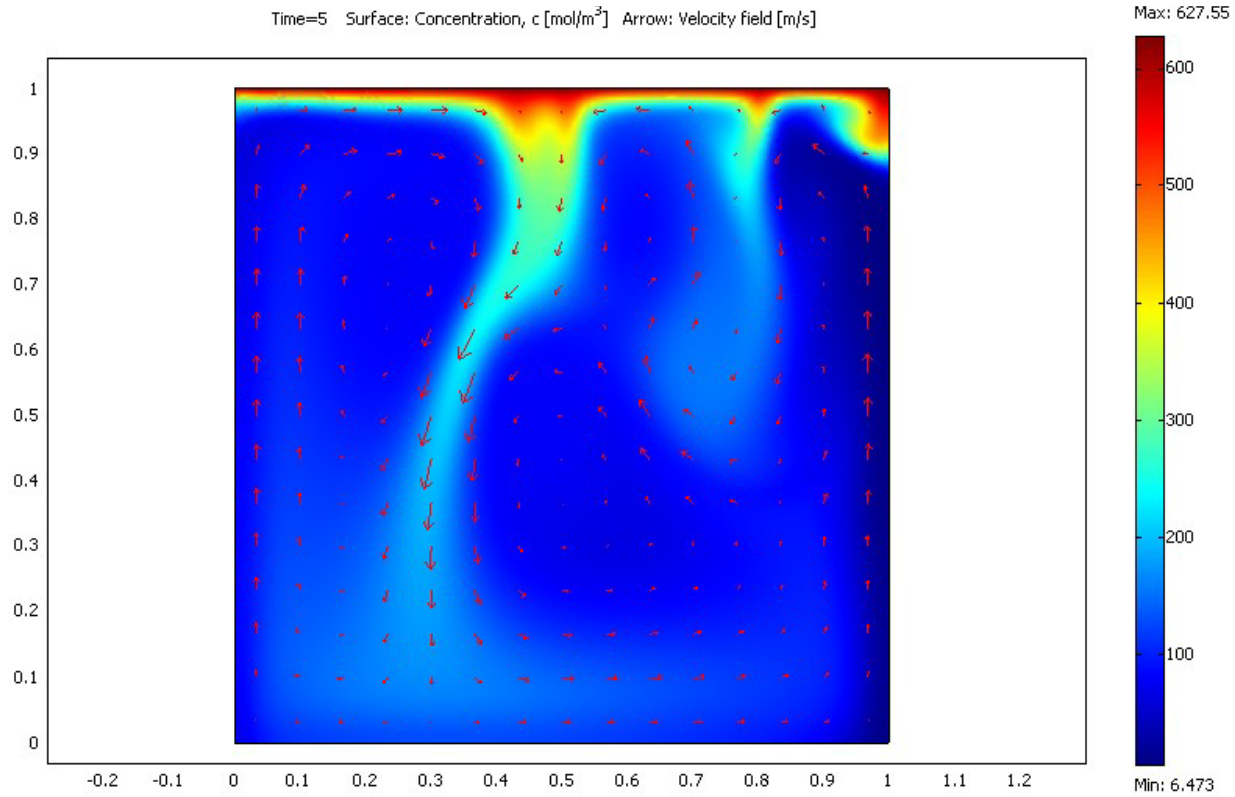

Figure 1
CO_2 Concentration Profile with Velocity Arrows at 5 minutes

Figure 1 illustrates the fluid behavior as CO_2 diffuses into the system causing the density of the solution to increase, which consequently causes the mixture to sink. In addition, there is a

reaction between the brine and the CO_2, which consumes the CO_2. As the CO_2-rich solution sinks to the bottom of the system, it mixes, diffuses and reacts away. These three processes are responsible for the concentration change seen along the streamlines as the system convects. This is best illustrated by the concentration profile change seen along both the central down-flow and along the flow that continues up the system sides.

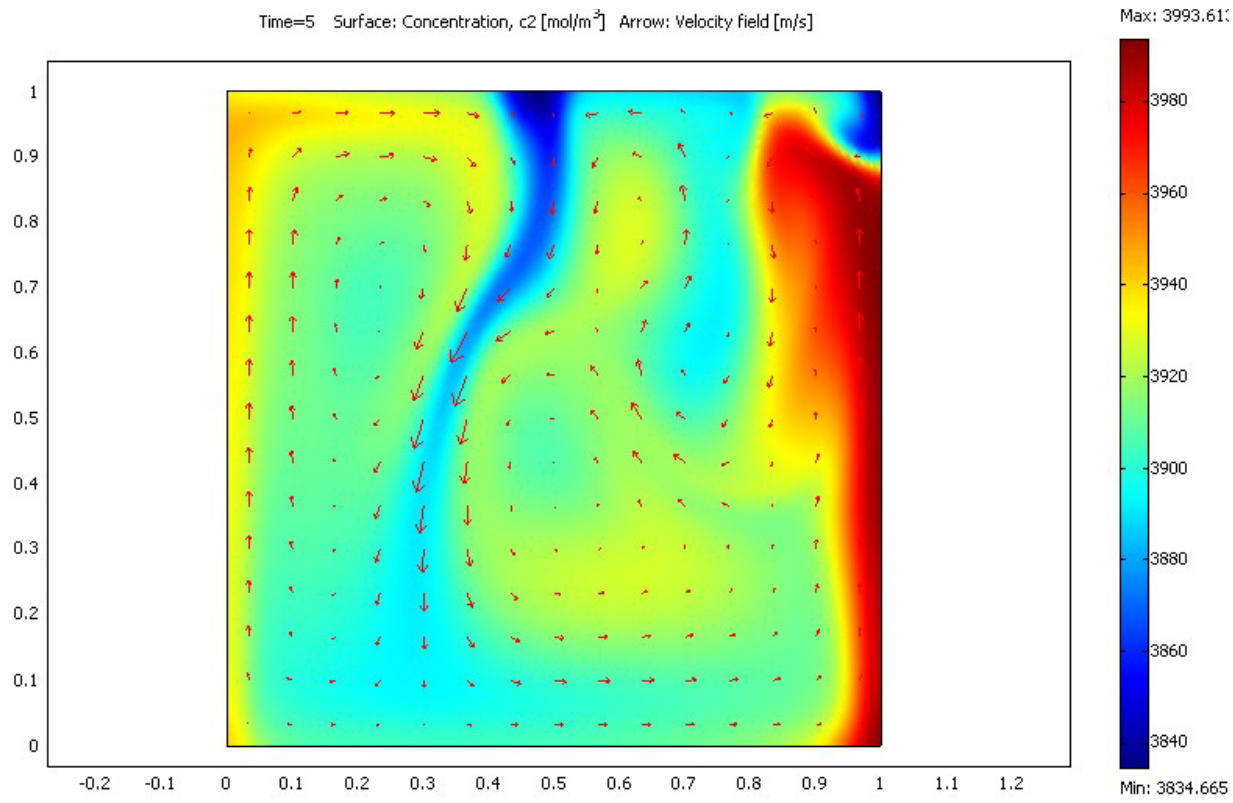

Figure 2
Brine Concentration Profile with Velocity Arrows at 5 minutes

Figure 2 illustrates the response of the brine to the influx, or injection, of CO_2. As CO_2 diffuses into the system the solution reacts with brine to reduce the brine concentration. The less concentrated brine/enriched-CO_2 fluid has increased density and sinks as a result. The less concentrated brine solution displaces the more concentrated brine solution as it moves from top to bottom, which is responsible for the blue region in the middle. This motion also forces highly concentrated brine to the surface as seen by the red region along the right side. The change in brine concentration is indicative of the chemical reaction occurring. With no reaction, the concentration profile remains constant at 4000 mol/m^3 regardless of how much CO_2 would diffuse into the system assuming that the total volume of the system does not change.

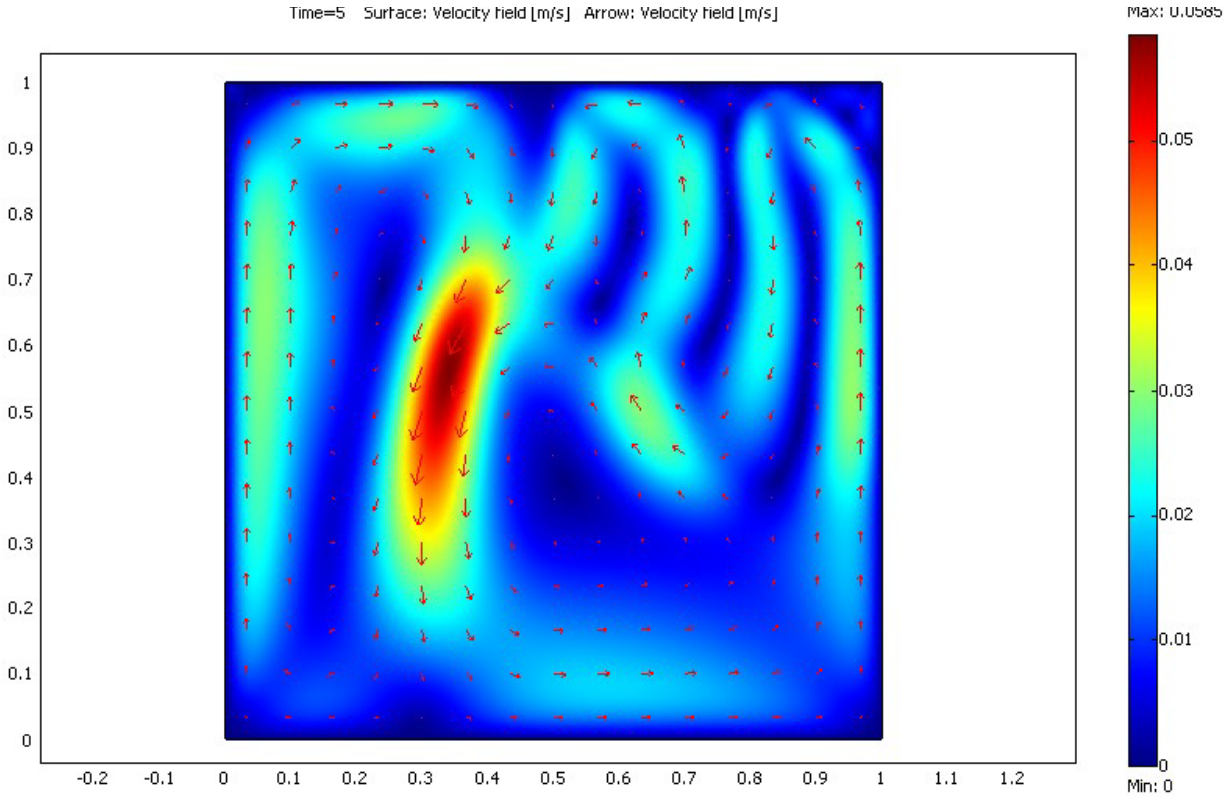

Figure 3
Velocity Field with Arrows at 5 minutes

Figure 3 indicates the convection cells that have formed as a result of the density driving forces. The high velocity profile in the center is a result of three convection cells merging that share a common down-flow. The effects of the no-slip condition applied as a boundary condition can also be seen as the velocity is zero around the perimeter of the system.

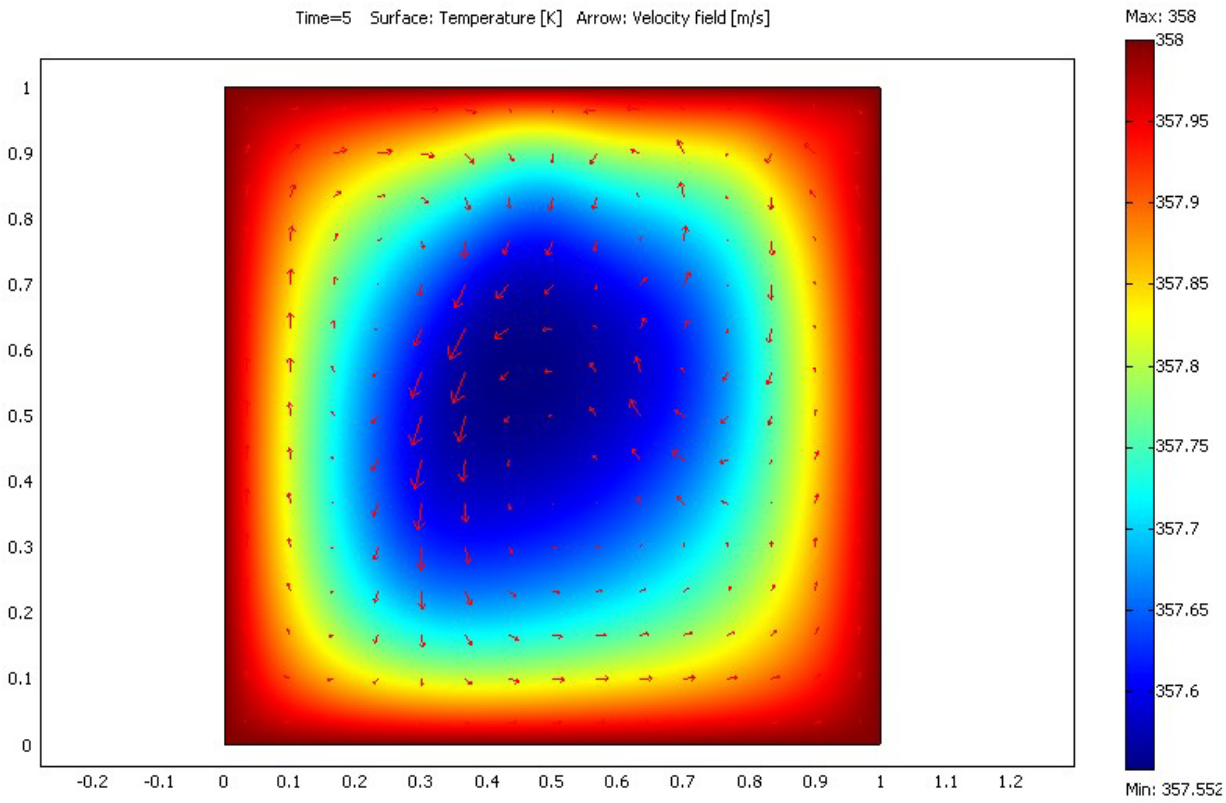

Figure 4
Temperature Profile with Velocity Arrows at 5 minutes

Figure 4 shows the temperature profile within the system. The calcite precipitation reaction is endothermic. Accordingly, the reaction does indeed proceed in this manner as the temperature drops within the system. Thermal conduction is evident within the system as heat flows in from the constant temperature boundaries that were imposed as initial conditions. The thermal conduction imposed on the system to generate a solution does not model reality. However, the behavior does give insight into how a coupled system would behave.

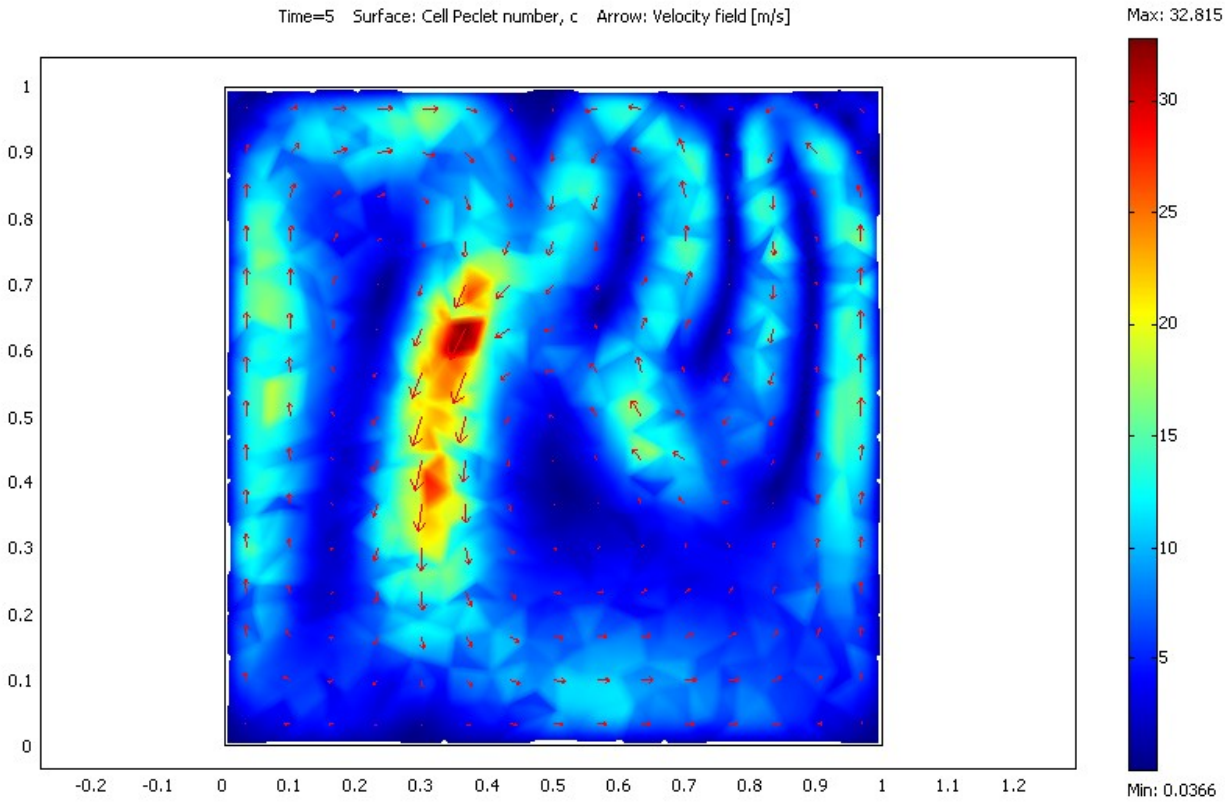

Figure 5
Concentration Peclet Number Profile with Velocity Arrows at 5 minutes

Figure 5 shows the concentration Peclet Number of the convection-diffusion equations within the system. Nominally, the Peclet Number should be less than 10. The Peclet number is the ratio of advective terms to diffusive terms. When the Peclet Number grows, relatively large velocity gradients exist, which are generally not linear. The solution may not be valid when this occurs because linear shape functions are generally applied. However, a Peclet number of 32 is not far from ideal, but could still be improved. The solution may not be entirely accurate but is close. A larger diffusion coefficient or smaller mesh size would result in a more favorable solution.

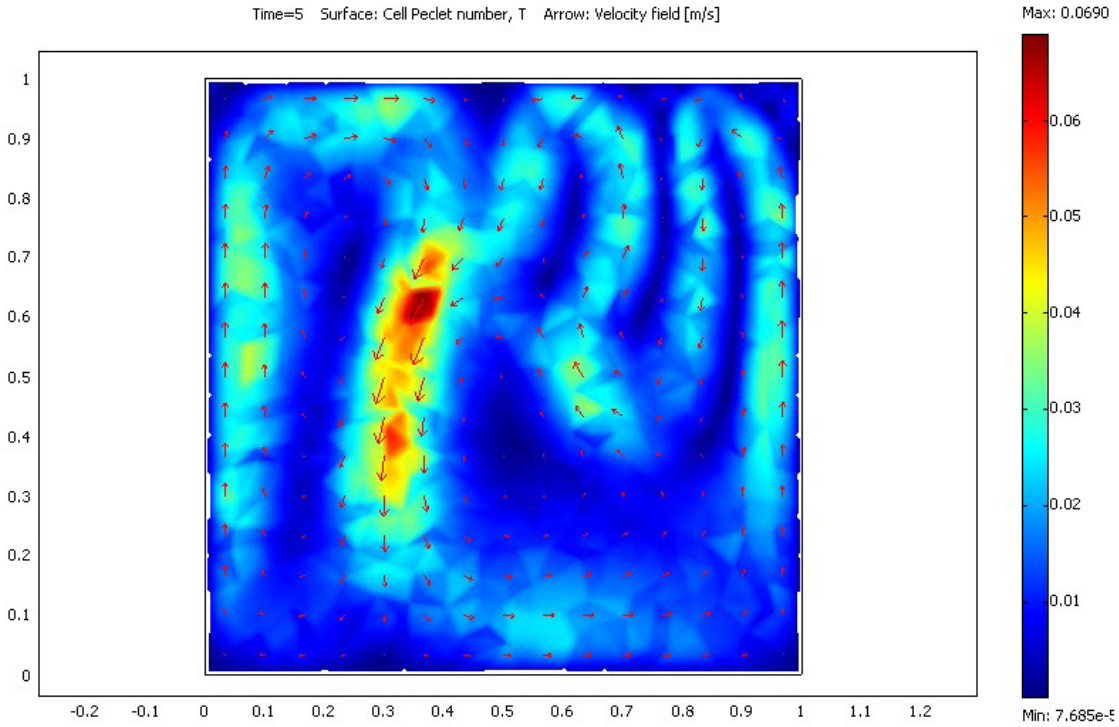

Figure 6
Temperature Peclet Number Profile with Velocity Arrows at 5 minutes

Figure 6 shows the conduction Peclet Number of the convection-conduction equations within the system. In this case, the Peclet Number is the ratio of advection to conduction. Here the conduction is sufficiently high enough to account for the velocity gradient.

VERIFICATION

The verification of a model is important in justifying the solution output of a given system. Three systems of equations describe the physical processes of CO_2 sequestration in deep saline aquifers including fluid flow, diffusion, and heat conduction. The equations used to describe these processes are the Navier-Stokes equations, advection-diffusion equations, and advection-conduction equations, respectively, and were combined to model fluid behavior in COMSOL 3.2. Each set of equations were evaluated in the modeling software and compared to known solutions.

The Navier-Stokes equations have been solved in cylindrical coordinates and are known to describe real fluid behavior in pipes. The velocity profile within a pipe as a function of radius can be described by the following equation:

$$V = \frac{\Delta P R^2}{4\mu L}\left(1 - \frac{r^2}{R^2}\right) \qquad (7)$$

From the Navier-Stokes equations, the slope of the pressure drop is found to be a constant and is a function of fluid properties and the pipe geometry. Equation 8 describes the pressure drop.

$$\frac{d\Delta P}{dL} = \frac{8\mu\bar{V}}{R^2} \qquad (8)$$

where V bar is the average velocity in m/s, ΔP is the change in pressure, L is the pipe length, μ is dynamic viscosity, and R is radius of the pipe. Using an average velocity of 1 m/s, a viscosity of 1 Pa-s, and a radius of 0.2m gives the slope to be 200 Pa/m. This slope was very closely matched in COMSOL 3.2 shown in Figure 7. The hook (circled) at the top-right is due to fluid entrance effects. Far from the entrance, the slope closely matches 200 Pa/m.

The profile given in Equation 7 was plotted in Figure 8 with ΔP/L=200 Pa/m, μ=1 Pa-s, and R=0.2 m. The velocity profile was also modeled with COMSOL 3.2 in Figure 9 assuming a pipe with R=0.2 m and L=6 m. Axial symmetry was used about r=0 and a no slip condition was applied at r=R. At z=0, a normal flow pressure condition of 0 Pa was applied. At z=6, an inflow velocity of -1 m/s was applied. Both Figures 8 and 9 show similar velocity profiles. Notice that the numerical solution (Figure 9) is very close but fails to reach the maximum velocity of 2 m/s. The maximum velocity given by COMSOL 3.2 was 1.979 m/s, which represents a 1.05% error. For most modeling work, this error is acceptable.

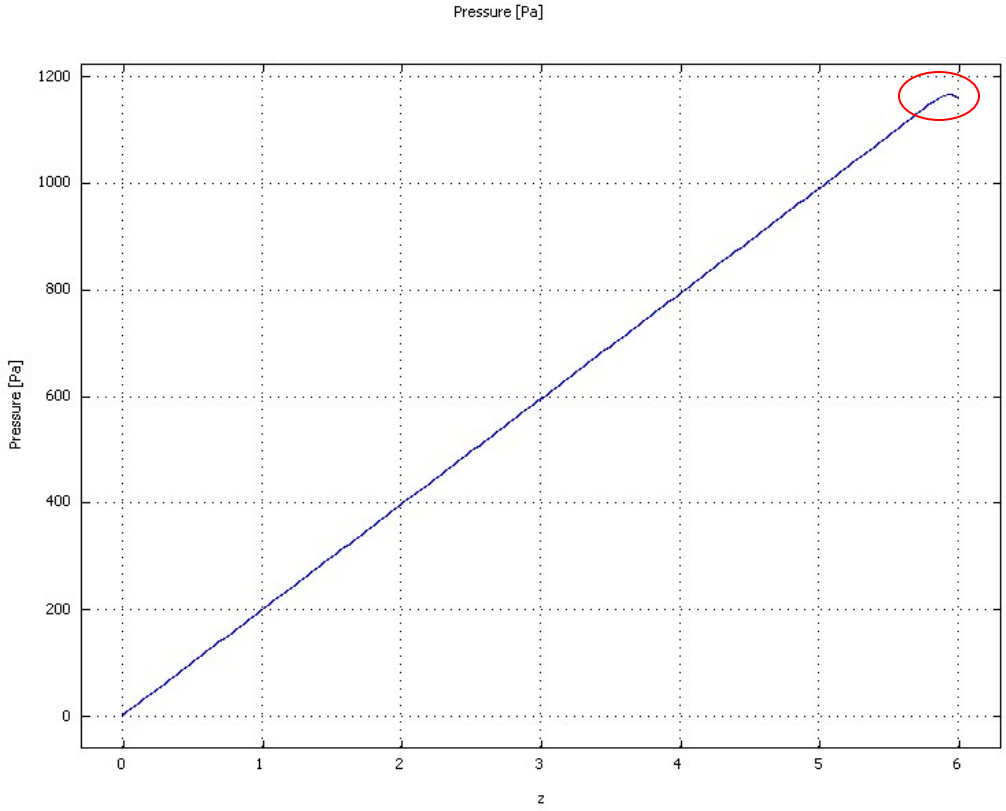

Figure 7
Pressure Drop as a Function of Length along the pipe Predicted by COMSOL 3.2

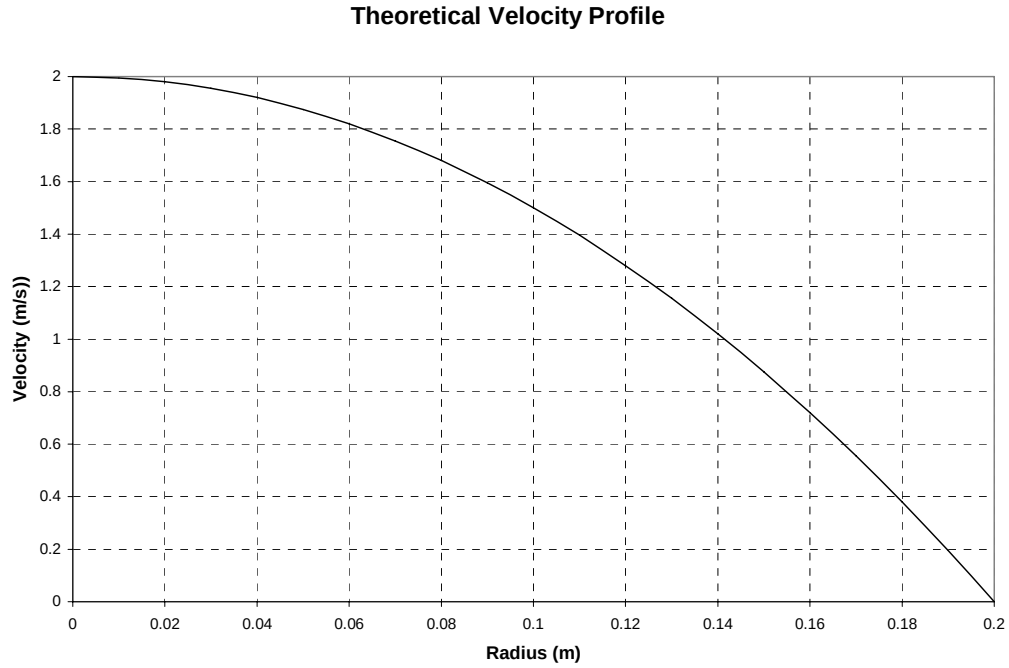

Figure 8
Velocity Profile predicted by Navier-Stokes for fluid flow in a Pipe

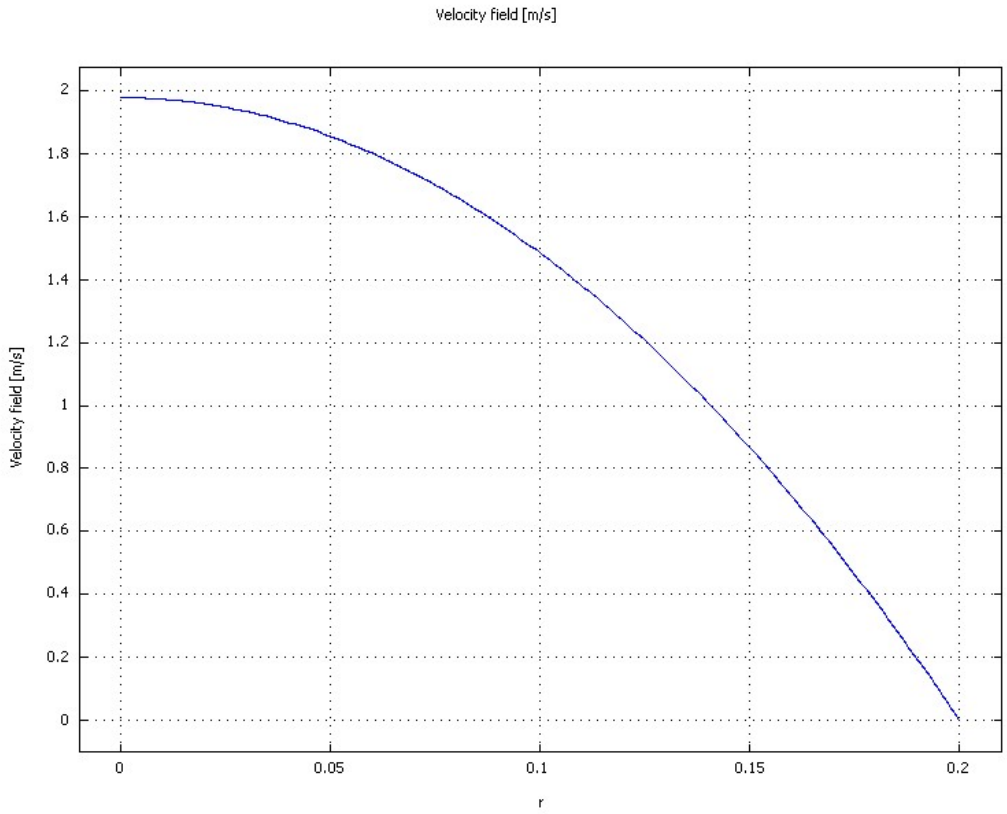

Figure 9
Velocity Profile Calculated from COMSOL 3.2 for Fluid Flow in a Pipe

The conduction and convection equations are essentially comparable. In 1-D, they can both be reduced to a similarity solution:

$$\frac{\partial \Psi^*}{\partial \tau} = \frac{\partial^2 \Psi^*}{\partial \delta^2} \qquad (9)$$

where $\Psi^*=C^*$ or $\Psi^*=T^*$, where $C^*=C/C_o$ and $T^*=T/T_o$ for the diffusion and conduction equations, respectively. Similarly, $\tau=Dt/L^2$ or $\tau=\kappa t/L^2$ respective to the equations, where D is the diffusion coefficient and κ is the thermal diffusivity in m^2/s. $\delta=x/L$ for both. When the equations are transformed in this manner, they collapse onto one single solution illustrated by Carslaw and Jaeger in Figure 10.

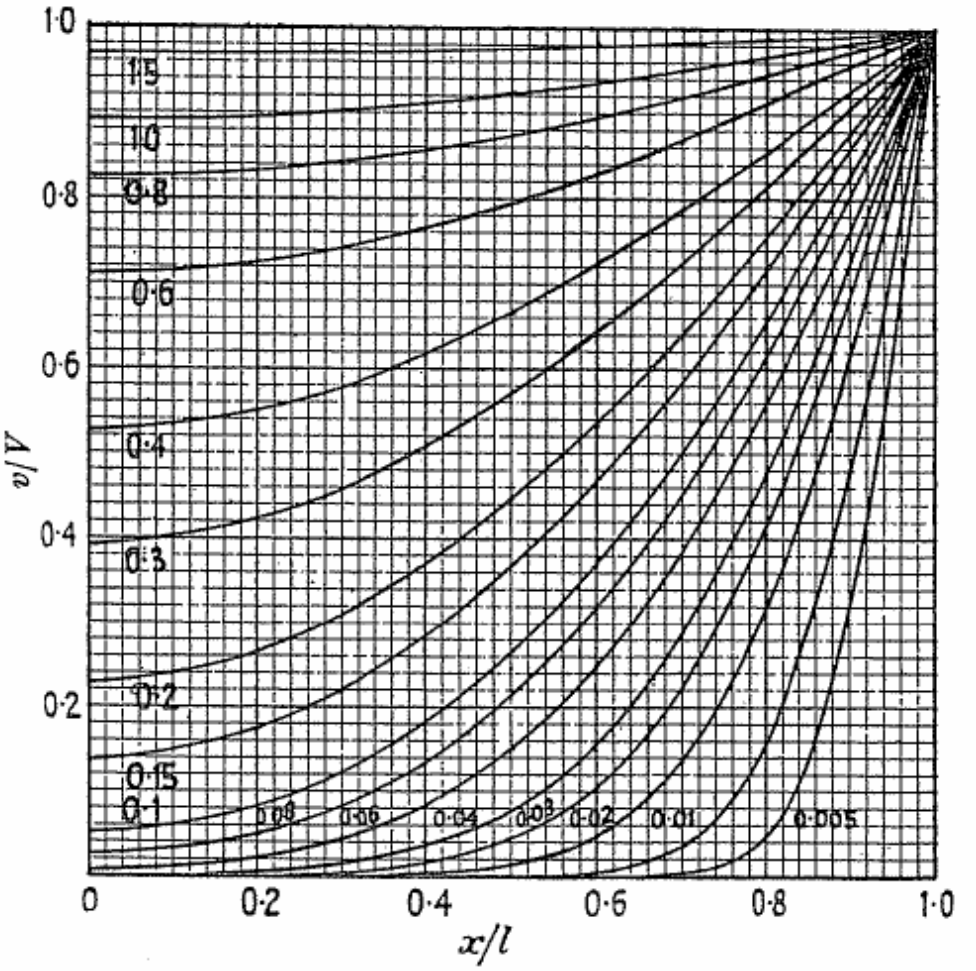

Figure 10 (from Carslaw and Jaeger)
Similarity Solution for Diffusion and Conduction $\Psi^*=v/V$, $\delta=x/l$, and the values on the chart represent τ

Figures 11 and 12 show the diffusion and conduction profiles given by COMSOL 3.2 when $C_o=T_o=1$, L=1, and $D=\kappa=1$. In both cases, the solutions from COMSOL 3.2 match the similarity solutions from Carslaw and Jaeger. This shows that the conduction and diffusion modules within COMSOL 3.2 are working properly. Each profile has a time-spacing of 0.05s between the successive lines and start 0.0s.

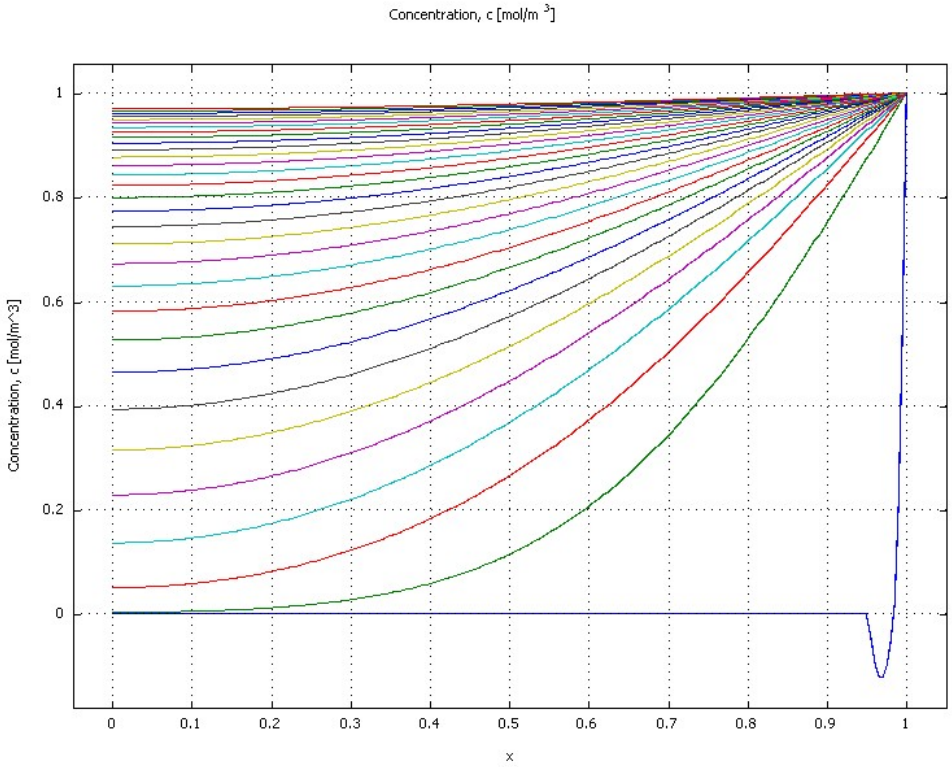

Figure 11
Time-dependent Diffusion Profiles from COMSOL 3.2

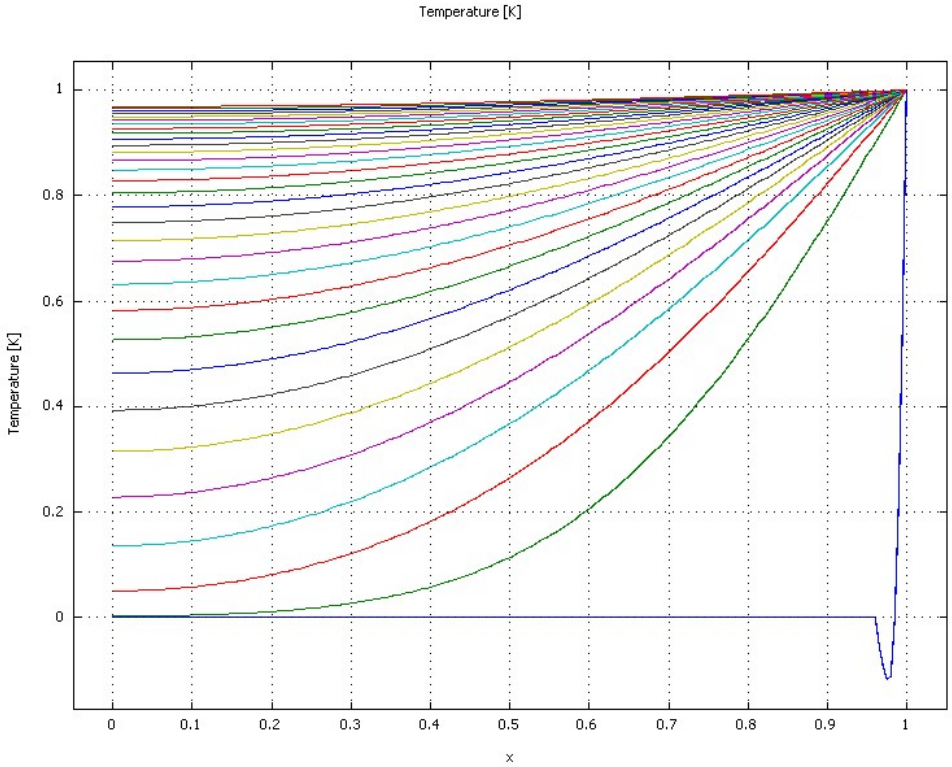

Figure 12
Time-dependent Conduction Profiles from COMSOL 3.2

The combination of advection with diffusion and conduction was evaluated by evaluating fluid flow between two plates with flux of material or heat into the system on a defined length. The advection should carry the fluid downstream and the conduction and diffusion should evenly spread the material and heat throughout the body of the fluid downstream. Figures 7 and 8 illustrate this principle in the modeling software. The flux was introduced in a 0.5m section of plate on the top and the bottom. The influx of material was set to 3.2mol/m^2 and the heat flow set to 1.6W/m^2. The mass and thermal diffusivity were set to 0.01m^2/s. The distance between the plates was set to 0.4m. All other parameters were set to unity. Appropriate boundary conditions of thermal and convective insulation were set to the plates except where flux was applied. The fluid inlet was set to 1 m/s with 0 concentration and temperature. The fluid outlet was set to normal flow with a pressure of 0Pa. Both inlet and outlet were allowed transport material or energy according to convection. Given these parameters, the downstream concentration would be expected to be 8mol/m^3 and the temperature to be 4 K.

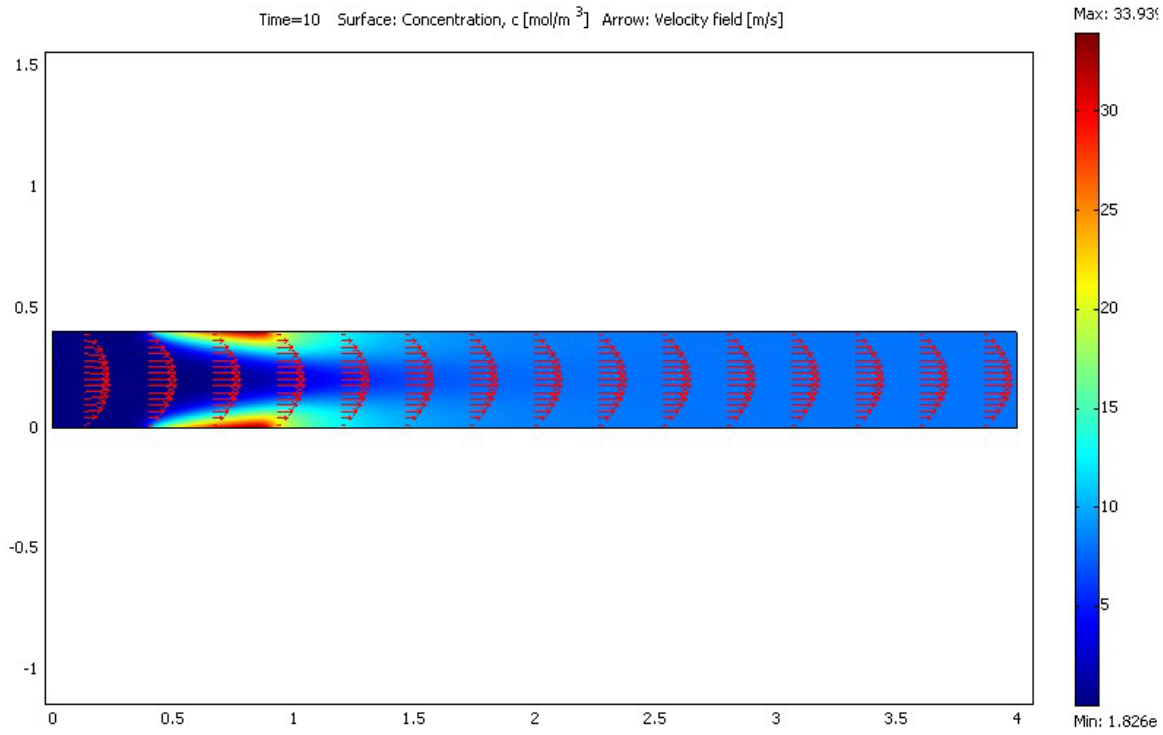

Figure 13
Verification of Diffusion-Advection in COMSOL 3.2

The downstream concentration was calculated to be 8.08 and the temperature to be 4.04. This represents a 1% error.

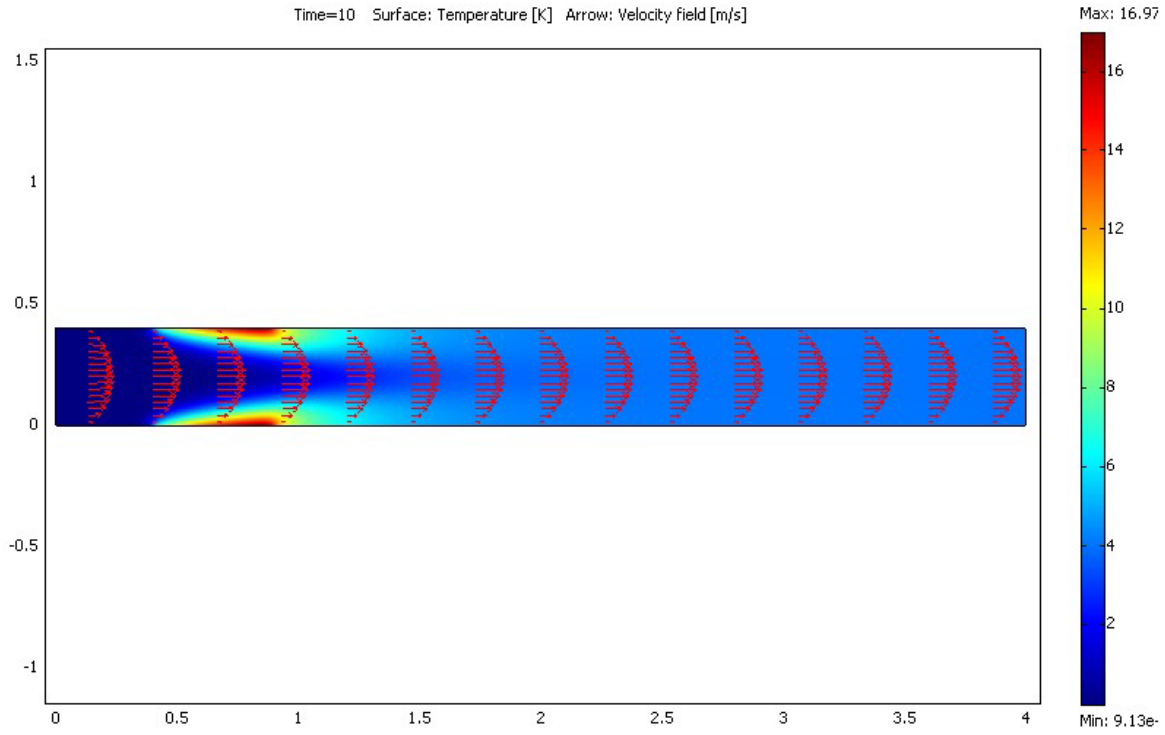

Figure 14
Verification of Conduction-Advection in COMSOL 3.2

A final verification check is that of reaction. The reaction of CO_2 with brine is an equilibrium surface reaction that is dependant on temperature, pressure, pH, concentration and particulate surface area. The scope of this study did not allow for the full incorporation of known kinetics, but rather for the incorporation of a simple first order, irreversible reaction. Thus the final state would be expected to have no brine and a concentration of CO_2 equal to that of the boundary concentration of 627.55mol/m^3. This was found to be the case within 1% error. Figures 15 and 16 show the time dependent concentration profiles along the bottom of the fluid cells.

The tests show that COMSOL 3.2 predicts behavior that is expected. There is little reason to believe that the software would not be able to accurately model real system behavior as long as the physical properties and supplemental math models (e.g., reaction, buoyancy, etc.) input into the program are accurate and representative of the real system. The software gives reasonable and accurate output for the equations that describe fluid motion, diffusion-advection, and conduction-advection.

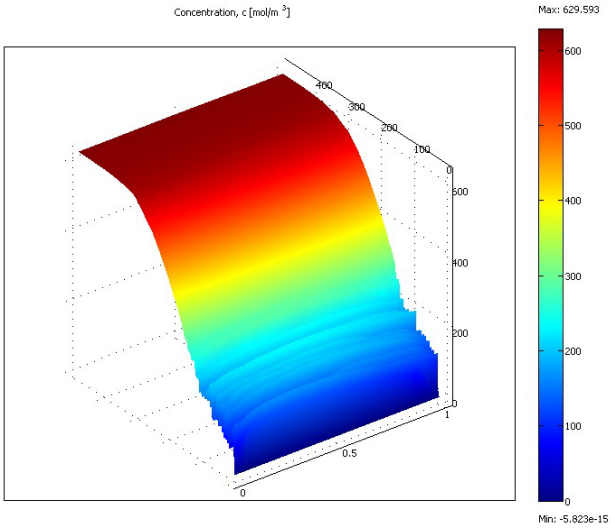

Figure 15
Time Dependent CO_2 Concentration Profile at the Lower Edge of the Cell
X=Length Along lower edge in Meters, Y=Time in Minutes, Z=Concentration in mol/m^3

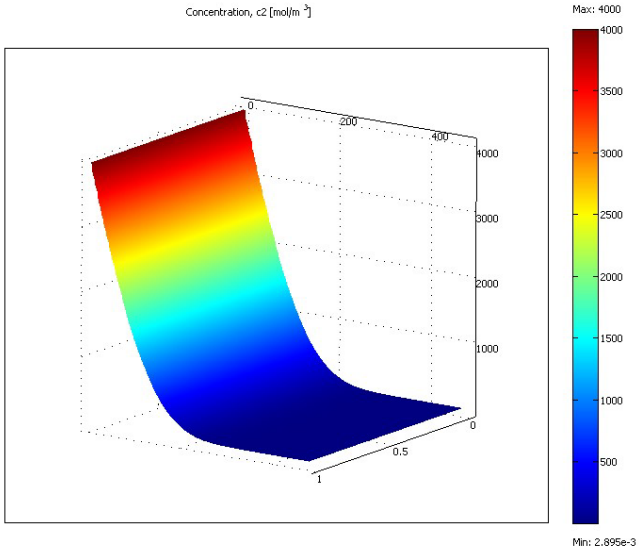

Figure 16
Time Dependent Brine Concentration Profile at the Lower Edge of the Cell
X=Length Along lower edge in Meters, Y=Time in Minutes, Z=Concentration in mol/m^3

PARAMETRIC STUDY

Three key parameters were identified that could greatly affect system behavior: the diffusion coefficient, the thermal conductivity, and the reaction constant. Figure 17 illustrates the behavioral change resulting from changes in the diffusion coefficient. Similarly, Figure 18 and Figures 19 and 20 illustrate behavioral changes when changes are made in thermal conductivity and reaction constant, respectively.

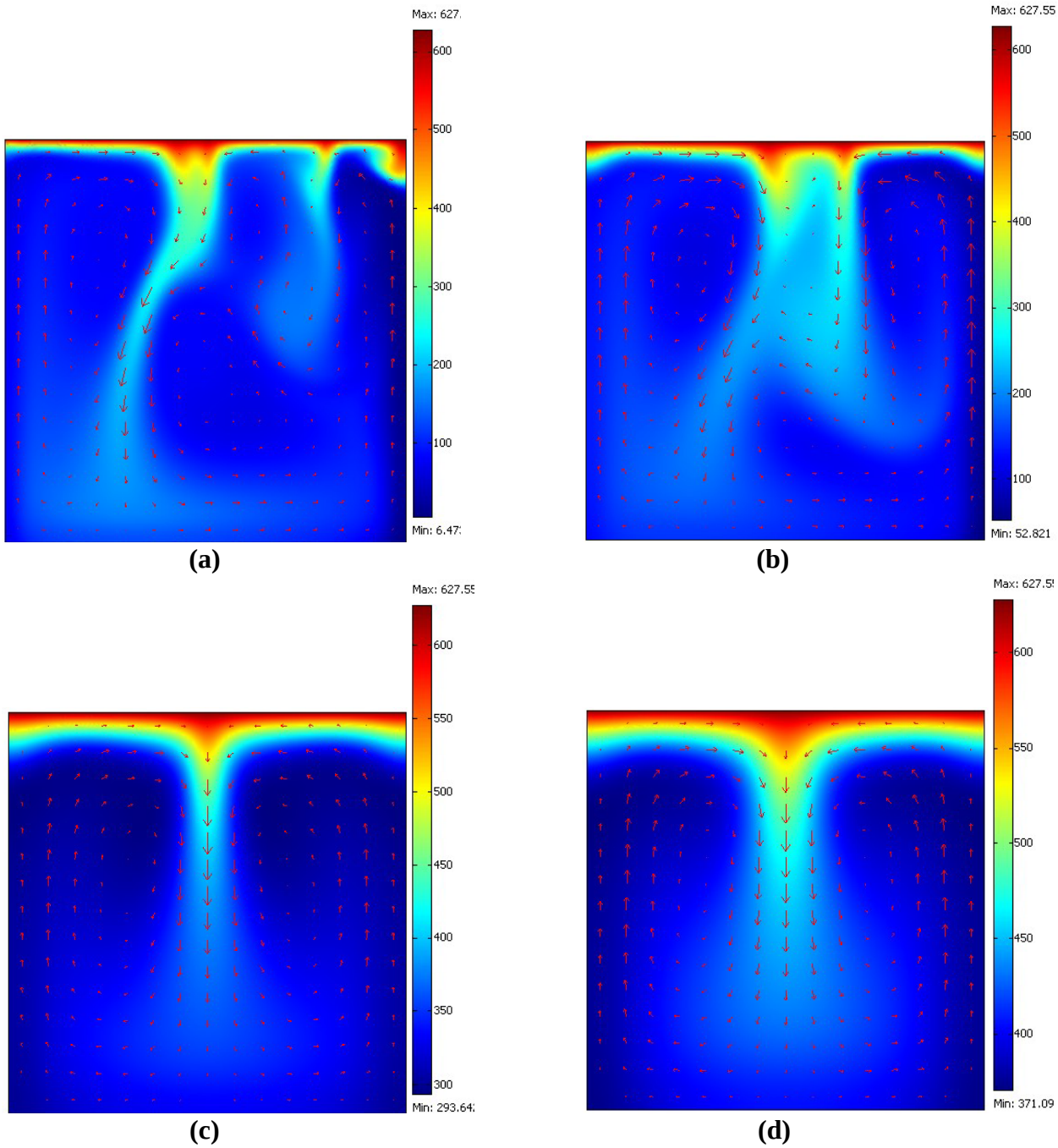

Figure 17
Parametric Study of Diffusion Coefficient: CO_2 Profile at time=5 min
(a) D=0.00005 (b) D=0.0001 (c) 0.0005 (d) 0.001

The diffusion coefficient strongly influences the influx of CO_2 and the formation of advection cells. When the diffusion coefficient is low, the CO_2-rich layer grows slowly and the gradient from lean to rich fluid is strong. This results in high instability, thus the layer cannot grow thick before advection begins. Because the layer is thin when advection initiates, the characteristic length that describes the width between the downdrafts, and thus the advection cells, is small. Several cells form initially; however, it is not stable to continue to have many cells at that length.

As time progresses, some of the advection cells merge as seen in Figure 17 (a) and (b). The remains of some of the original downdrafts can be seen as "spikes" in the said figures. When the diffusion coefficients are large, the initial layer grows thick and the resulting downdrafts are separated by a characteristic length that does not allow for the development of more than a single, stable, and central downdraft within the cell.

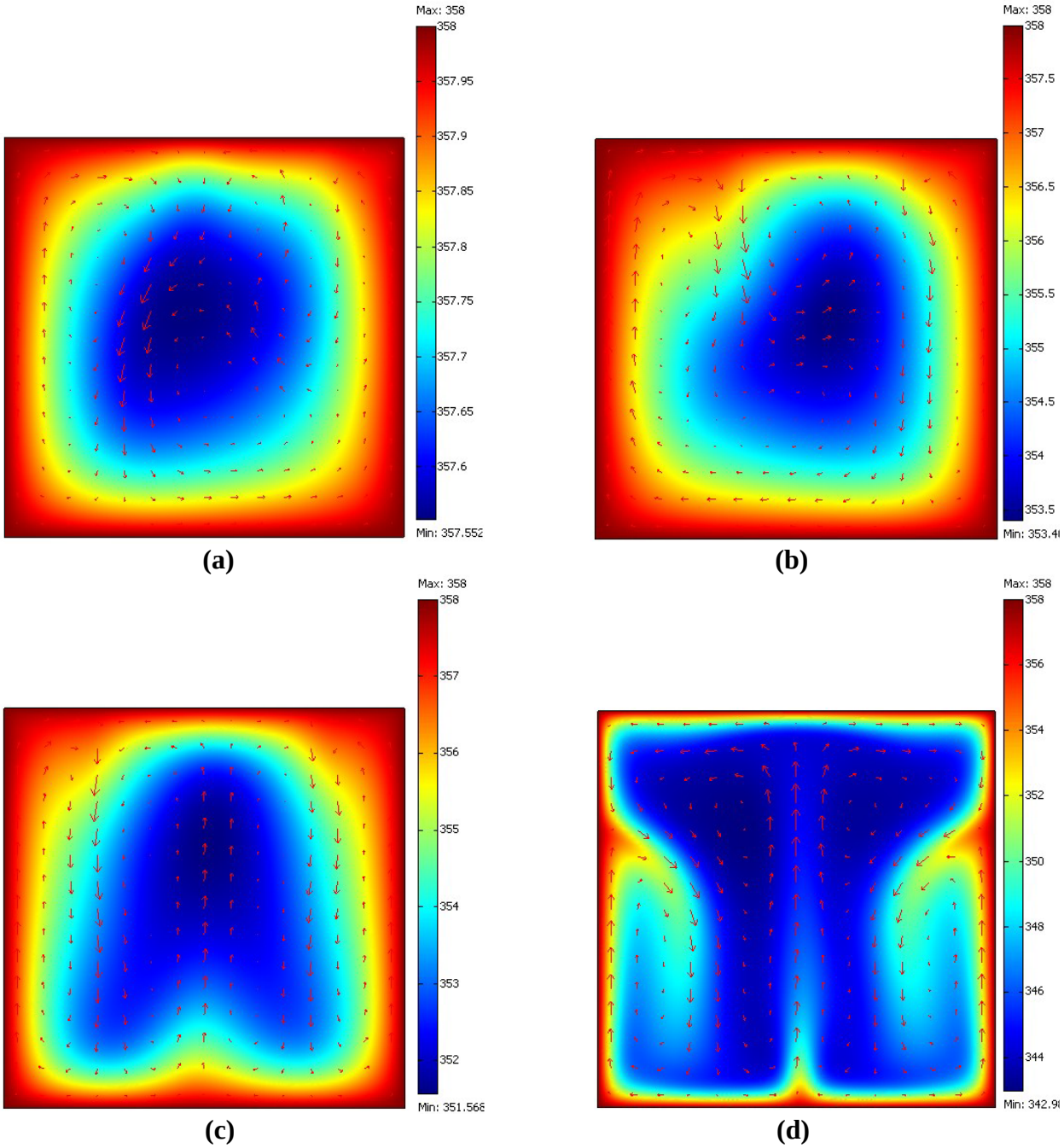

Figure 18
Parametric Study of Thermal Conductivity: Temperature Profile at time=5 min
(a) tc=100000 (b) tc=10000 (c) tc=5000 (d) tc=500

The thermal conductivity has been shown to have a large effect on the advection and the temperature profile as shown in Figure 18. As expected, the temperature gradients grow stronger and the minimal temperature drops as the thermal conductivity decreases. This has profound impacts on the circulation because the temperature differential provides driving force for circulation through thermal expansion. As the thermal conductivity drops, the circulation along the sides grows stronger. Several circulation cells develop, rather than two roughly symmetric cells.

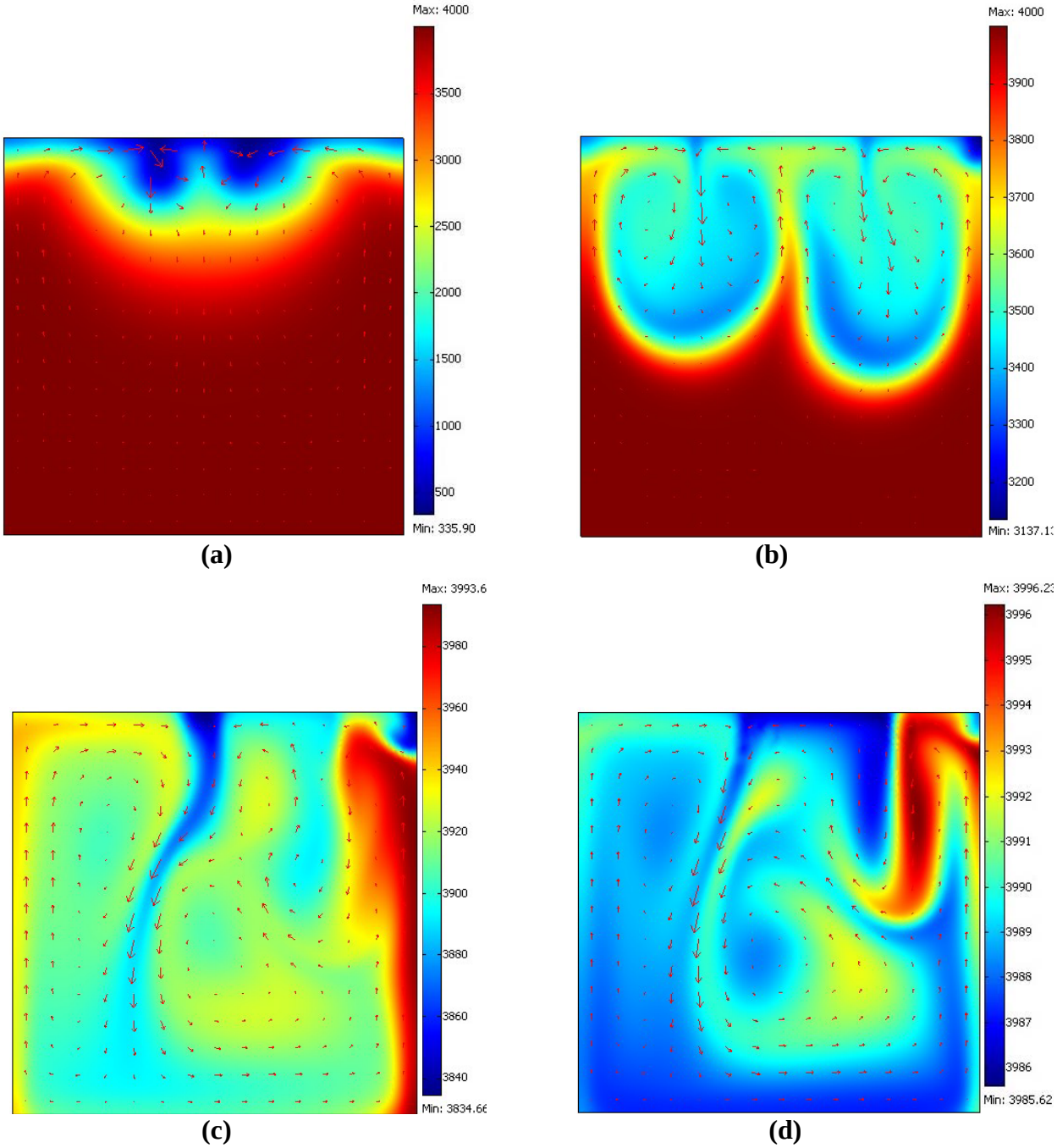

Figure 19
Parametric Study of Reaction Constant: Brine Profile at time=5 min
(a) k=0.0001 (b) k=0.00001 (c) k=0.000001 (d) k=0.0000001

The reaction coefficient strongly impacts the properties of the system. Most predominant, is the impact on the concentration gradient. As the reaction slows, the concentration gradient lessens. In addition, at any given time, the minimum brine concentration grows higher. When reaction grows quite fast, the initial diffusion layer has difficulty growing as the CO_2 reacts away. This retards the development of advection currents as seen in Figure 19 (a) and (b). Once the reaction slows enough, the general circulation pattern begins to stabilize with respect to reaction rate as seen in (c) and (d).

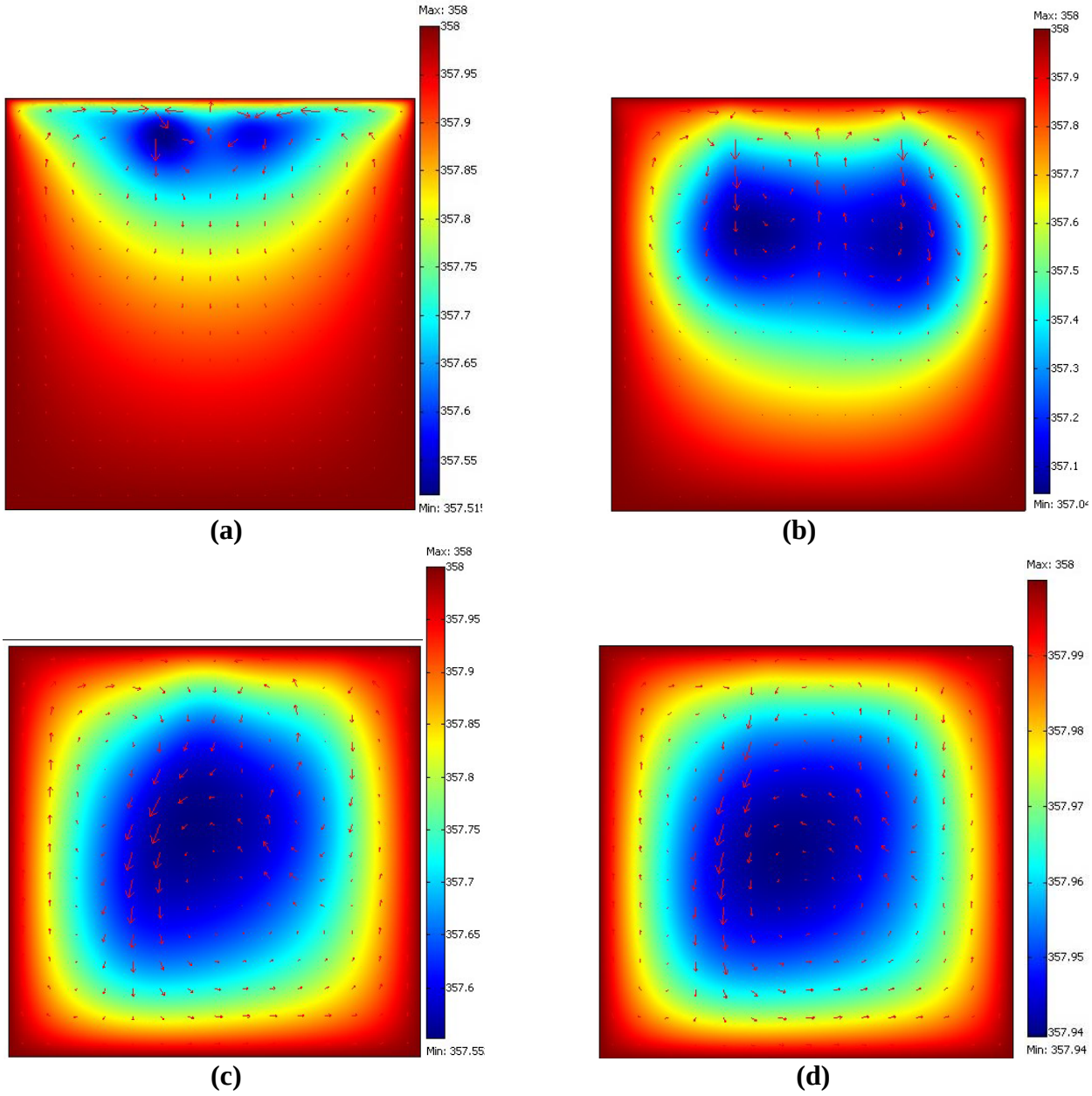

Figure 20
Parametric Study of Reaction Constant: Temperature Profile at time=5 min
(a) k=0.0001 (b) k=0.00001 (c) k=0.000001 (d) k=0.0000001

The final effect that the speed of reaction has is the place at which the reaction occurs. When the reaction is fast, the reaction takes place only at areas where the concentration gradients are strong

(i.e., there is a boundary developed between reacted products and reactants). This can most strongly be seen in Figure 19 and 20 (a). As the reaction slows, the boundary lessens and the reaction can occur more or less as the same rate throughout the entire body. This can be seen by the relatively constant and stable temperature gradients that develop seen in Figure 20 (a) and (b).

CONCLUSIONS

The shear amount of CO_2 emissions today, and the expected future growth, is and will continue to be a problem. A viable solution is the sequestration of CO_2 in saline aquifers. The two predominant sequestration mechanisms, solubility and mineral trapping, were modeled in this study. The behavior was approximated within a two dimensional square with sides of one meter. The advection-diffusion, Navier-Stokes, and advection-conduction equations were combined with reaction, concentration, and thermal body forces to model the behavior. The behavior could not be accurately modeled within the time and computing resources of this course. However, the behavior attained was reasonable given the constraints. Given more resources, the actual behavior could be closely modeled.

REFERENCES

1. Keeling, C.D. and T.P. Whorf, *Atmospheric CO_2 records from sites in the SIO air sampling network. In Trends: A Compendium of Data on Global Change*. 2005, Carbon Dioxide Information Analysis Center, Oak Ridge National Laboratory, U.S. Department of Energy: Oak Ridge, Tenn.

2. Portier, S. and C. Rochelle, *Modelling CO2 solubility in pure water and NaCl-type waters from 0 to 300 degrees C and from 1 to 300 bar - Application to the Utsira Formation at Sleipner.* Chemical Geology, 2005. **217**(3-4): p. 187-199.

3. Soong, Y., et al., *Experimental and simulation studies on mineral trapping of CO2 with brine.* Energy Conversion and Management, 2004. **45**(11-12): p. 1845-1859.

4. Van der Meer, L.G.H., *Investigations regarding the storage of carbon dioxide in aquifers in the Netherlands.* Energy Conversion and Management, 1992. **33**: p. 611-618.

5. Koide, H., et al., *Subterranean Containment and Long-Term Storage of Carbon-Dioxide in Unused Aquifers and in Depleted Natural-Gas Reservoirs.* Energy Conversion and Management, 1992. **33**(5-8): p. 619-626.

6. Holloway, S., *Underground sequestration of carbon dioxide - a viable greenhouse gas mitigation option.* Energy, 2005. **30**(11-12): p. 2318-2333.

7. Gunter, W.D. and E.H. Perkins, *Aquifer Disposal of Co2-Rich Gases - Reaction Design for Added Capacity.* Energy Conversion and Management, 1993. **34**(9-11): p. 941-948.

8. Krom, T.D., F.L. Jacobsen, and K.H. Ipsen, *Aquifer Based Carbon-Dioxide Disposal in Denmark - Capacities, Feasibility, Implications, and State of Readiness.* Energy Conversion and Management, 1993. **34**(9-11): p. 933-940.

9. Vanderburgt, M.J., J. Cantle, and V.K. Boutkan, *Carbon-Dioxide Disposal from Coal-Based Igccs in Depleted Gas-Fields.* Energy Conversion and Management, 1992. **33**(5-8): p. 603-610.

10. Hendriks, C.A. and K. Blok, *Underground-Storage of Carbon-Dioxide.* Energy Conversion and Management, 1993. **34**(9-11): p. 949-957.

11. Saylor, B.Z. and B. Zerai, *Injection and trapping of carbon dioxide in deep saline aquifers. Energy, Waste, and the Environment: a Geochemical Perspective.* 2004. **236**: p. 285-296.

12. Gunter, W.D., E.H. Perkins, and I. Hutcheon, *Aquifer disposal of acid gases: modelling of water-rock reactions for trapping of acid wastes.* Applied Geochemistry, 2000. **15**(8): p. 1085-1095.

13. Allen, D.E., et al., *Modeling carbon dioxide sequestration in saline aquifers: Significance of elevated pressures and salinities.* Fuel Processing Technology, 2005. **86**(14-15): p. 1569-1580.

14. Druckenmiller, M.L. and M.M. Maroto-Valer, *Carbon sequestration using brine of adjusted pH to form mineral carbonates.* Fuel Processing Technology, 2005. **86**(14-15): p. 1599-1614.

15. O'Connor, W.K., et al., *Aqueous Mineral Carbonation, Mineral Availability, Pretreatment, Reaction Parametrics, and Process Studies*. 2004, Albany Research Center. p. 1-19.

16. Bachu, S., W.D. Gunter, and E.H. Perkins, *Aquifer Disposal of Co2 - Hydrodynamic and Mineral Trapping.* Energy Conversion and Management, 1994. **35**(4): p. 269-279.

17. Kaszuba, J.P., D.R. Janecky, and M.G. Snow, *Carbon dioxide reaction processes in a model brine aquifer at 200 degrees C and 200 bars: implications for geologic sequestration of carbon.* Applied Geochemistry, 2003. **18**(7): p. 1065-1080.

18. Herzog, H., *What future for carbon capture and sequestration?* Environmental Science & Technology, 2001. **35**(7): p. 148a-153a.

19. Oldenburg, C.M., et al., *Mixing of stably stratified gases in subsurface reservoirs: A comparison of diffusion models.* Transport in Porous Media, 2004. **54**(3): p. 323-334.

20. Webb, S.W. and K. Pruess, *The use of Fick's law for modeling trace gas diffusion in porous media.* Transport in Porous Media, 2003. **51**(3): p. 327-341.

21. Sato, T. and K. Sato, *Numerical prediction of the dilution process and its biological impacts in CO2 ocean sequestration.* Journal of Marine Science and Technology, 2002. **6**(4): p. 169-180.

22. Gaus, I., M. Azaroual, and I. Czernichowski-Lauriol, *Reactive transport modeling of the impact of CO2 injection on the clayey cap rock at Sleipner (North Sea).* Chemical Geology, 2005. **217**: p. 319-337.

23 Orr, F.M., 2001. *Diffusion of CO_2 during hydrate formation.* Presented at: Multiscale Reservoir Investigations and Applications to Terrestrial CO_2 Sequestration Symposium. Held: December 7-8, 2001.

24 Lide, D.R., 2002. CRC Handbook 83rd Edition. CRC Press: 2664 pages.

25 Zhang, Y. and R. Dawe, 1998. *The kinetics of calcite precipitation from a high salinity water.* Applied Geochemistry **13**: p. 177-184.

26 Duan, Z. and R. Sun, 2003. *An improved model calculating CO_2 solubility in pure water and aqueous NaCl solutions from 273 to 533 K and from 0 to 2000 bar.* Chemical Geology **193**: p. 257-271.

27 The Physics Hypertextbook, 2005. *Thermal Expansion*. [cited 2005 October 26th]; Available from: http://hypertextbook.com/physics/thermal/expansion/.

28 Yang, C. and Y. Gu, 2005. *Accelerated mass transfer of CO_2 in reservoir brine due to density-driven natural convection at high pressures and elevated temperatures.* Industrial & Engineering Chemistry Research **(In Publication)**.